

Ultrasonically facilitated two-dimensional crystallization of colloid particles

著者	羽根 一博
journal or publication title	Journal of applied physics
volume	80
number	9
page range	5427-5431
year	1996
URL	http://hdl.handle.net/10097/35565

doi: 10.1063/1.362730

Ultrasonically facilitated two-dimensional crystallization of colloid particles

Minoru Sasaki^{a)} and Kazuhiro Hane

Department of Mechatronics and Precision Engineering, Tohoku University, Sendai 980-77, Japan

(Received 3 January 1996; accepted for publication 26 July 1996)

A new ultrasonic radiation technique is described which facilitates the ordering of colloid particles into regular two-dimensional arrays. Ultrasonic radiation during the evaporation of the colloid solution enlarges the area of the particulate array and leads to a densely packed lattice reducing voids and random assemblies. Lattices of polystyrene particles (diameter: 64, 137, and 330 nm) and gold particles (diameter: 39 nm) were prepared under various ultrasonic powers. The arrays were imaged by the scanning electron microscope or the atomic force microscope. © 1996 American Institute of Physics. [S0021-8979(96)04421-0]

I. INTRODUCTION

There has been considerable interest in preparing two-dimensionally ordered colloid crystals due to their potential applications (e.g., lithography,¹ optical units,² microelectronics, and information storage). An ordered array of identical colloid particles can be regarded as a nanometer-scale analogy of the atomic lattice with the advantage that one can manipulate arbitrary particles under the ambient condition³ using the atomic force microscope (AFM).⁴

The simplest way to pack the colloid particles is by spreading a drop of the suspension on a substrate and letting it dry. With this open-air system it is difficult to produce a large area of ordered structure from submicrometer sized particles. A number of preparation methods has been developed to control the ordering process and to improve the quality of the array. In early works, a two-dimensional structure of polystyrene spheres was formed at an air-water interface,⁵ and then transferred onto the solid substrate using the Langmuir-Blodgett approach.⁶ Sheppard and Tchekedjian investigated the use of organic liquids and amphiphilic molecules adsorbed onto latex particles which helped the spreading of the particles over the water surface to form the monolayer film.⁷ Deckman *et al.* presented a spin coating technique which required optimized parameters (e.g., spin speed, rheology of the sol, volume fraction, and substrate surface chemistry) for each particle size.⁸ Denkov *et al.* created a promising method which used a ring to reverse the meniscus profile of the solution from convex to concave.⁹ Crystal growth started from the ring center and progressed toward its periphery to give a closely packed lattice. Giersig and Mulvaney employed electrophoretic deposition to prepare ordered monolayers of gold particles, which were stabilized by the surfactant coat to prevent reduction.¹⁰

In this article, we present an ultrasonic radiation method for improving the quality of two-dimensional arrays of colloid particles, and compare them with those produced without ultrasonic radiation. Four suspensions of two different colloid materials (polystyrene and gold) are employed.

II. EXPERIMENT

A. Materials

Polystyrene and gold particles were purchased as suspensions in pure water. The polystyrene latex solutions were prepared by diluting the original suspensions with distilled water. The gold colloid solution was used without dilution. Table I lists the characteristic parameters of the solutions. The mean diameters of the colloid particles were 330, 137, 64, and 39.0 nm.

We used a glass cover slip (Matsunami, diameter: 15 mm) as a convenient substrate. The cover glass was soaked in ethanol and then wiped dry with cheesecloth. This glass substrate was used for the polystyrene particles. For the gold particles, the glass surface was etched with ~5 % HF solution for ~1 min to improve the hydrophilicity of the substrate.

B. Deposition

Figure 1 shows a schematic diagram of the ultrasonic radiation device, which consists of an ultrasonic humidifier (Toyotomi, model TUH-4 is modified for higher power) filled with water and the tin vial. A few drops of the suspension were pipetted onto the glass substrate, and then dried while being ultrasonically irradiated in the ambient laboratory air. The initial 5 μ l drop spread over an area (~40 mm²) and formed a convex meniscus as shown in Fig. 1(a). The ultrasonic waves (frequency: 2.4 MHz) traveled from the piezoelectric radiator through the water medium to the vial. The vial was positioned so that the wetting solution was directly irradiated by the ultrasonic beam. The initial drop was dried within 30 min. For the deposition of the 64 nm sized polystyrene and the 39 nm sized gold particles, Teflon rings⁹ (diameter: 6 and 4 mm, respectively) were incorporated into the device as shown in Fig. 1(b).

C. Metal coat

The polystyrene particle arrays were plasma coated with Os (thickness: 5 nm) to permit observation by the scanning electron microscope (SEM) and to improve the mechanical stability of the particles for the AFM scan. It is known that

^{a)}Research Fellow of the Japan Society for the Promotion of Science; Electronic mail: sasaki@hane.mech.tohoku.ac.jp

TABLE I. Characteristic parameters of the solutions and experimental techniques. The standard deviation of the size distribution is shown as a percentage of the mean diameter. The numbers in the Note column refer to makers (1: Nisshin EM Co., Ltd.; 2: Polyscience, Inc.; 3: British Biocell International). Additional experimental techniques used are denoted by the letters (r: in combination with a Teflon ring, h: HF treatment to make the glass substrate hydrophilic).

Material	Mean diameter (nm)	Standard deviation (%)	Volume fraction (%)	Initial volume (μl)	Note
Polystyrene	330	1.2	0.1	5.0	1
Polystyrene	137	12	0.04	5.0	1
Polystyrene	64	15	0.02	5.0	2,r
Gold	39.0	<20	0.0003	2.5	3,r,h

isolated particles are swept aside by the AFM stylus, and that the resulting image does not show the sample shape, but shows some lines along the fast scan direction (fleeting image).^{3,11,12} These lines are traces of the tip movement as it moves the particle around the surface. When the packing of particles is poor, the situation is similar to that of isolated particles. The Os coat is expected to fix the particle to the substrate and to prevent the particle from rolling out of the scan area.

D. Imaging

The larger 330 nm sized particles were examined using a SEM (Hitachi, Ltd., S-2250N). The accelerating voltage was 25 kV, which was the maximum value obtained with this microscope. The smaller 64 and 39 nm sized particles were measured using a handmade AFM.¹³ Imaging was in contact mode. Commercial cantilevers (Park Scientific Instruments) with a spring constant of $0.031 \pm 0.003 \text{ N/m}$ were used.

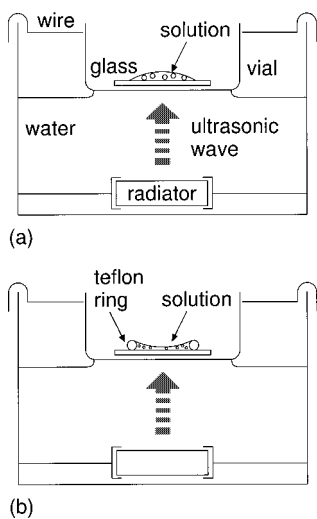


FIG. 1. Schematic diagram of the experimental setup for deposition with ultrasonic radiation. The circular piezoelectric radiator (diameter: 1.6 cm) is ~ 4 cm from the bottom of the tin vial (diameter: 4 cm and thickness: 1.5 cm). The water temperature can increase from ~ 18 to ~ 30 °C when the ultrasonic humidifier works at high power (≥ 68 W). The humidity of the laboratory air is not controlled.

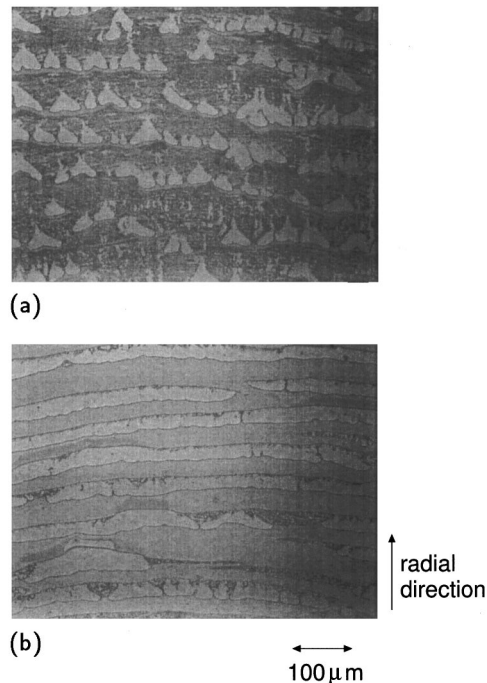


FIG. 2. Optical micrographs of depositions of 137 nm sized polystyrene particles prepared (a) without and (b) with ultrasonic radiation (power: 39 W). There are trends in the borderline of the colored stripe. The radially outside borderline has some notches and faces to the clear empty space. The radially inside one is smooth and there are some ripple aggregations in its neighborhood.

III. RESULTS

Representative experimental results are described, since the results for all particles were similar.

A. Deposition

The colloid deposits were observed with an optical microscope ($\times 100$) using reflected light. Figure 2 shows optical micrographs of typical views when 137 nm sized polystyrene particles are prepared (a) without and (b) with the ultrasonic radiation (power: 39 W, the value referring to the power consumption of the ultrasonic humidifier). Figure 2(a) shows black ripples of particulate aggregations, which are formed at the transient periphery of the droplet. While the water is evaporating, particles are carried in the radial direction towards the liquid periphery. Figure 2(a) includes some different regions, which are narrow (width: $\sim \mu\text{m}$) and evenly light blue. These colored stripes are expected to be ordered arrays.¹⁴ Such regions are rare in the deposited area. When the sample is prepared while being ultrasonically irradiated, the colored stripes become larger (width: 10–100 μm and length: $\sim \text{mm}$) and distributed over the deposited area. The ripple aggregation becomes minor. Figure 2(b) shows typical stripes surrounded by empty spaces. Although there are some apparently random variations from run to run, the efficacy of the ultrasonic wave in enlarging the colored region seems to be proportional to its power. As the particle size decreases, the area of the striped region decreases and the higher powered ultrasonic wave becomes necessary. Above 77 W, however, the tin vial and its fixing wire vibrate strongly and the ordering is ruined.

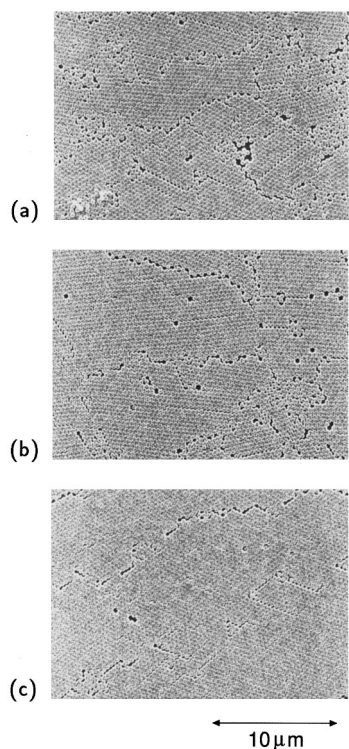


FIG. 3. A series of SEM images of 330 nm sized polystyrene particle monolayers obtained with various ultrasonic radiation powers (a) 0, (b) 39, and (c) 59 W. Images cover the almost full width of the obtained colored stripes. The size distribution of this particle is sharpest of our experimental samples, and the hexagonal regularity is most obvious.

The color of the stripes is due to interference at two parallel interfaces (air-polystyrene and polystyrene-glass). The different colors accord with the respective thicknesses of the ordered layers. The light blue color corresponds to the monolayer of 137 nm sized polystyrene particles.¹⁵ Most of the striped regions are light blue and so are monolayers. Figure 2(b) also includes some multilayers which are iridescently colored (yellow, yellow green, orange, and so on) regions.

Table I includes the volume fractions used. In the case of the polystyrene particles, thicker solutions simply produce larger colored areas which include multilayers as well as monolayers. As the ultrasonic power increases, the width of each stripe begins to saturate, however, use of the ring technique permits the development of much broader stripes ($\sim 500 \mu\text{m}$). In the case of the gold particles, metallic colored stripes (width: $5\text{--}10 \mu\text{m}$ and length: $\sim \text{mm}$ along the ring circumference) are formed. These stripes have some regions with discretely different reflectances. It was found necessary to minimize the radiation time by reducing the initial volume of the solution. When the gold colloid solutions were ultrasonically irradiated for prolonged periods ($>1 \text{ h}$), dark red flocs, which are considered to be aggregations of gold particles, grow and disturb the formation of the regular structure.

B. Images

Figures 3(a)–3(c) show SEM images of the monolayers of 330 nm sized spheres obtained with various ultrasonic

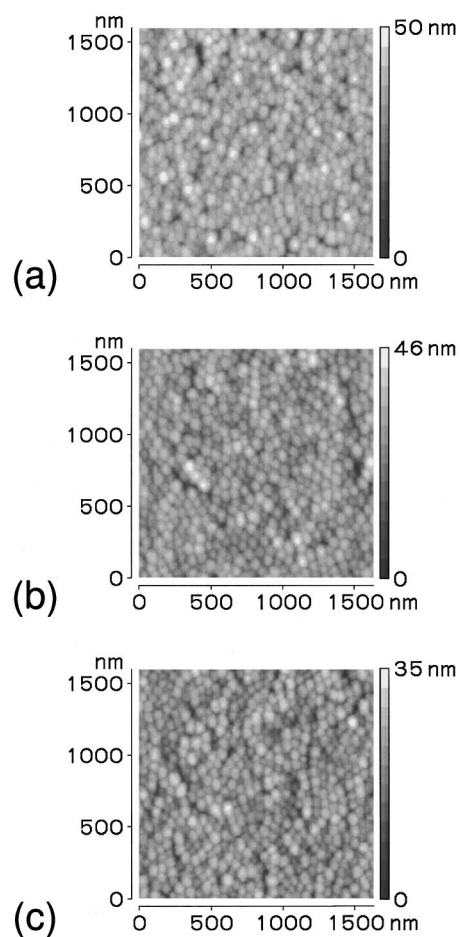


FIG. 4. A series of AFM images of 64 nm sized polystyrene particles at the middle of the monolayer stripes obtained with various ultrasonic radiation powers (a) 0, (b) 39, and (c) 68 W. The intermediate force is $\sim 4 \text{ nN}$. The scan speed is $\sim 1 \text{ Hz}$. Images are stored as 150×150 point arrays. We calibrate the movement of the x and y piezo scanners from the AFM image of the array of 330 nm sized particles.

radiation powers (0, 39 and 59 W, respectively). The colored stripes correspond to the regions of close packing of the particles. There are some domains with a hexagonal lattice, and they are usually separated by narrow gaps or random assemblies which sometimes have a second layer of particles on them. The narrow (subparticle diameter width) lines are quadratic structures of the array. The number of such defects decreases and the area of hexagonal domains increases, as the ultrasonic power increases from Fig. 3(a) to Fig. 3(c). The regular lattice is seen as a softly undulating surface interrupted in places by holes corresponding to missing particles. Figure 3(c) shows that the ordering periodicity persists over $\sim 20 \mu\text{m}$. Although there are some narrow gaps in the film, a uniform direction of the hexagonal lattice is nearly maintained.

Figures 4(a)–4(c) are AFM images of the monolayer of 64 nm sized particles obtained with various ultrasonic radiation powers (0, 39, and 68 W, respectively). Due to the broad particle size distribution, the film shows a mosaic lattice instead of a hexagonal one. The size difference between particles is obvious. The lattice quality of Fig. 4(b) is improved compared with that of Fig. 4(a). There are large and deep

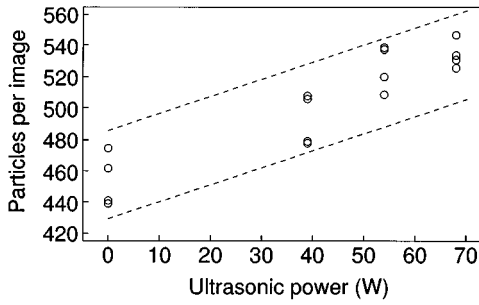


FIG. 5. The number of 64 nm sized particles included in the AFM images ($1599 \times 1636 \text{ nm}^2$) as a function of the ultrasonic power. All borderline particles are counted as a half. If a perfect hexagonal lattice of 64 nm sized identical spheres is considered, the observed area would theoretically include 737 particles.

voids all over the film obtained using the single ring technique alone without ultrasonic radiation. The lattice obtained using only ultrasonic radiation technique is also loose. The combination of both the ring and ultrasonic radiation techniques gives a better quality of lattice than that obtained using either one of the techniques alone. The packing density of the particle increases from Fig. 4(a) to Fig. 4(c). There are 476, 508, and 547 particles in Figs. 4(a)–4(c), respectively. Figure 5 shows the number of particles included in the film image with variation in ultrasonic radiation power. Four images were selected randomly and evaluated for each sample. Although there is some variation, the particle numbers clearly increase with the ultrasonic power (~ 1.1 particle per W on average). The more densely packed lattices are considered to show smaller particle sizes in the AFM image. Since the tip radius of $\sim 20 \text{ nm}$ is comparable with the particle size, the convolution of the tip profile creates the artificial broadening of the particle images so hiding small voids. The films of Fig. 4(a) or Fig. 4(b) may have more small voids than that of Fig. 4(c) in reality.

Gold particles are more stable than the polystyrene particles to the scanning of the AFM probe, and an image can be obtained without the Os coat. Figure 6 shows AFM images of the bare monolayer of 39 nm sized gold particles obtained (a) without and (b) with ultrasonic radiation (power: 68 W). Figure 6(a) includes large voids and second layer particles, which are larger than the first layer particles in appearance. As seen from Fig. 6(b), the film quality of the gold particle is again improved by ultrasonic radiation. When the packing is poor or the scanning is done many times, the gold particle layer begins to show some “fleeting” parts in the image. The hydrophilic treatment of the glass substrate is effective in reducing voids or aggregations and makes the area of the particulate arrays larger.

IV. DISCUSSION

Slowing of the evaporation rate is a well-known method for improving the array quality. Although the drying speed does not change very much in bulk suspension, the ultrasonic waves induce the atomization of water¹⁶ and the drying process becomes faster than that in open air. This difference is most obvious when the Teflon ring is used. Since the ring

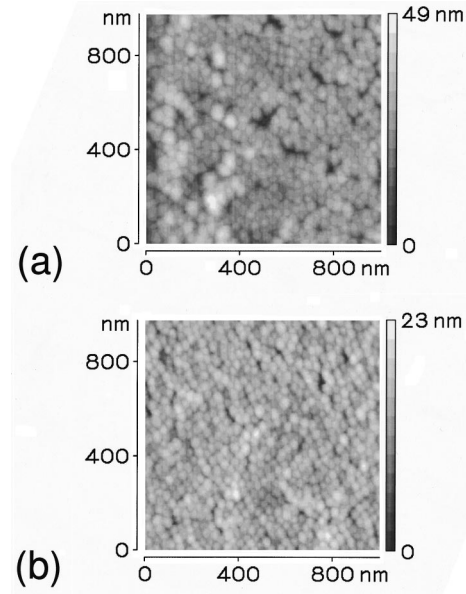


FIG. 6. AFM images of gold particles at the monolayer stripes prepared (a) without and (b) with ultrasonic radiation (power: 68 W).

prevents the evaporation of water in the gap between the ring and the substrate, it takes more than 1 h to dry the solution. Ultrasonic radiation reduces the drying time to less than 30 min. The ultrasonic wave works in a different way from that of the slow evaporation method. Possible reasons why the ultrasonic wave improves the quality of the two-dimensional array will be connected with the dynamic process of the array growth mechanism, where the driving forces are the convective water flux and the attractive lateral capillary force.^{9,17–19} The ordering process is thought to consist of the following three stages.

(i) The first step is nucleation when the thickness of the water layer becomes approximately equal to the particle diameter. Some domains of an ordered phase appear, and attract each other to form the nucleus.

(ii) The second step is crystal growth. Figure 7 shows a schematic diagram of the following two stages. The water evaporation from the already ordered nucleus induces the water flux in that direction from the disordered bulk suspension toward the ordered nucleus. This water flux carries new particles which continuously attach to the nucleus periphery and allows crystal growth. Since the attenuation of the ultrasonic wave is proportional to the volume fraction of the solution, its effect may be dominant in the condensed phase.²⁰ The ultrasonic wave further facilitates water evaporation in the condensed regions, which are originally dominant, and

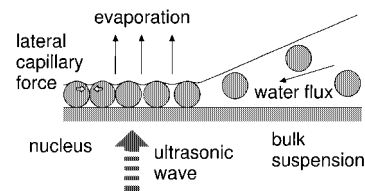


FIG. 7. Schematic presentation of the ordering process of the particle driven by the water flux and the attractive lateral capillary force.

thereby increases the intensity of the convective particle influx. More colloid particles are thus transported across the substrate to the nucleus. The fact that the attenuation of the ultrasonic wave decreases as the diameter of the polystyrene particle decreases may explain why a higher power of ultrasonic wave is necessary for the smaller particle.

(iii) The third step is the compression of the loose lattice after the particle spreading has finished. This annealing process is not reported in the usual case of solid substrates (e.g., glass and mica),^{9,17,19} but is seen on liquid substrates (e.g., mercury and fluorinated oil).^{18,21} Lazarov *et al.* obtained an improved result using a fluorinated oil substrate by decreasing the water vapor pressure,²¹ which also increased the evaporation rate of water. Ultrasonically induced force may disrupt the relatively weak interactions (particle–substrate and particle–particle) and rearrange particles in the film. If the remaining water in the array can evaporate, increased deformation of the water meniscus will take place to produce higher interparticle attractions. Particles can be rearranged by these forces to form more densely packed lattices. When the sample is continuously ultrasonically irradiated for ~1 h, even after the solution has apparently dried, the AFM image stability of the bare layer is improved compared with that of samples stored in a desiccator for several days.

V. CONCLUSIONS

We have described a new ultrasonic irradiation preparation method which improves the quality of two-dimensional colloid particulate arrays. Ultrasonic radiation is a dynamic method which does not affect the nature of the particle, and is thus different from surfactant techniques. Well-ordered two-dimensional arrays covering large areas can be obtained with sufficient ultrasonic power. This approach is effective for both polystyrene and gold particles and may be applicable to other colloid materials or substrates.

ACKNOWLEDGMENTS

The authors gratefully acknowledge K. Nagayama, Tokyo University, for his informative suggestions on the order-

ing process of colloid particles. The ultrasonic humidifier was kindly provided by M. Sato, Honda Electronics Corporation. The Os coat was prepared with the help of Nippon Laser & Electronics Laboratory Corporation.

- ¹J. C. Hulsteen and R. P. V. Duyne, *J. Vac. Sci. Technol. A* **13**, 1553 (1995).
- ²S. Hayashi, Y. Kumamoto, T. Suzuki, and T. Hirai, *J. Colloid Interface Sci.* **144**, 538 (1991).
- ³T. Junno, K. Deppert, L. Montelius, and L. Samuelson, *Appl. Phys. Lett.* **66**, 3627 (1995).
- ⁴G. Binnig, C. F. Quate, and Ch. Gerber, *Phys. Rev. Lett.* **56**, 930 (1986).
- ⁵P. Pieranski, *Phys. Rev. Lett.* **45**, 569 (1980).
- ⁶J. W. Goodwin, R. H. Ottewill, and A. Parentich, *J. Phys. C* **84**, 1580 (1980).
- ⁷E. Sheppard and N. Tcheurekdjian, *J. Colloid Interface Sci.* **28**, 481 (1968).
- ⁸H. W. Deckman and J. H. Dunsmuir, *Appl. Phys. Lett.* **41**, 377 (1982); H. W. Deckman, J. H. Dunsmuir, S. Garoff, J. A. McHenry, and D. G. Peiffer, *J. Vac. Sci. Technol. B* **6**, 333 (1988).
- ⁹N. D. Denkov, O. D. Velev, P. A. Kralchevsky, I. B. Ivanov, H. Yoshimura, and K. Nagayama, *Nature (London)* **361**, 26 (1993).
- ¹⁰M. Giersig and P. Mulvaney, *Langmuir* **9**, 3408 (1993).
- ¹¹B. Schleicher, T. Jung, and H. Burtscher, *J. Colloid Interface Sci.* **161**, 271 (1993).
- ¹²T. Junno, S. Anand, K. Deppert, L. Montelius, and L. Samuelson, *Appl. Phys. Lett.* **66**, 3295 (1995).
- ¹³M. Sasaki, K. Hane, S. Okuma, M. Hino, and Y. Bessho, *Rev. Sci. Instrum.* **65**, 3697 (1994).
- ¹⁴E. Adachi, A. S. Dimitrov, and K. Nagayama, *Langmuir* **11**, 1057 (1995).
- ¹⁵C. D. Dushkin, K. Nagayama, T. Miwa, and P. A. Kralchevsky, *Langmuir* **9**, 3695 (1993).
- ¹⁶M. G. Sirotyuk, *Sov. Phys. Acoust.* **8**, 165 (1962); T. K. McCubbin, Jr., *J. Acoust. Soc. Am.* **25**, 1013 (1953).
- ¹⁷C. D. Dushkin, H. Yoshimura, and K. Nagayama, *Chin. Phys. Lasers* **204**, 455 (1993).
- ¹⁸A. S. Dimitrov, C. D. Dushkin, H. Yoshimura, and K. Nagayama, *Langmuir* **10**, 432 (1994).
- ¹⁹N. D. Denkov, O. D. Velev, P. A. Kralchevsky, I. B. Ivanov, H. Yoshimura, and K. Nagayama, *Langmuir* **8**, 3183 (1992).
- ²⁰J. R. Allegra and S. A. Hawley, *J. Acoust. Soc. Am.* **51**, 1545 (1972); J. W. Povey and M. G. Scanlon, *J. Colloid Interface Sci.* **93**, 565 (1983).
- ²¹G. S. Lazarov, N. D. Denkov, O. D. Velev, P. A. Kralchevsky, and K. Nagayama, *J. Colloid Interface Sci.* **90**, 2077 (1994).